Chemical Engineering Journal 162 (2010) 677–684

Contents lists available at ScienceDirect

Chemical Engineering Journal

journal homepage: www.elsevier.com/locate/cej

Adsorptive removal of Cr (VI) by Fe-modified activated carbon prepared from *Trapa natans* husk

Weifeng Liu, Jian Zhang*, Chenglu Zhang, Yifu Wang, Ye Li

Shandong Key Laboratory of Water Pollution Control and Resource Reuse, School of Environmental Science and Engineering, Shandong University, Jinan 250100, China

ARTICLE INFO

Article history:
Received 11 April 2010
Received in revised form 12 June 2010
Accepted 14 June 2010

Keywords:
Adsorption
Fe-modified activated carbon
Trapa natans husk
Cr (VI)

ABSTRACT

Fe-modified activated carbon (THAC-Fe) was developed from a low-cost aquatic plant residue, *Trapa natans* husk, and tested for its ability to remove Cr (VI) from aqueous solutions. The surface characteristics of the carbons before and after modification were measured. The results showed that impregnation with Fe increased the carbon surface area, introduced more acidic functional groups, and improved the adsorption ability by nearly three times as compared to the original activated carbon. The effects of solution pH, adsorbent dose, contact time and initial Cr (VI) concentration on the adsorption of Cr (VI) by THAC-Fe were investigated. The adsorption capacity decreased sharply with the increase of solution pH. The kinetics data followed the pseudo-second-order model and the rate of chromium (VI) uptake was found to be controlled by external mass transfer and intra-particle diffusion throughout the entire adsorption period. Boyd plot confirmed that film diffusion was the rate-limiting step in the adsorption process. Equilibrium data fit well to the Tempkin and Freundlich models. The maximum adsorption capacity was 11.83 mg/g at room temperature as calculated by Langmuir equation. According to the calculated thermodynamic parameters, the adsorption was a spontaneous endothermic process. Since Cr (VI) cannot be easily desorbed using distilled water or NaOH solutions, chemisorption is the likely mode of adsorption. According to these results, THAC-Fe is a promising adsorbent for the removal of Cr (VI) from wastewater.

1. Introduction

Hexavalent chromium, Cr (VI), is one of the most dangerous inorganic water pollutants in terms of its carcinogenic and mutagenic effects and its toxicity to the liver.

It is widely distributed in the wastewater from the dyes, pigments, metal cleaning, plating, leather and mining industries [1], thus forms a great threat to surface and groundwater quality. Removal of Cr (VI) from wastewater can be accomplished by various purification techniques including electro-deposition [2], membrane filtration [3], ion exchange [4], adsorption [5], and biological processes [6]. However, many of these processes are not widely practiced due to their disadvantages including incomplete metal removal, requirements for expensive equipment and monitoring systems, or generation of toxic sludge or other waste products that require disposal [7]. Adsorption has proved to be an effective and reliable method for the removal of toxic heavy metals from wastewater. Activated carbon is the most widely used absorbent today, owing to its highly developed porosity, excellent adsorption capacity and high degree of surface reactivity [8]. However, commercially available activated carbons are usually expensive due to their high-cost sources, and this restricts their extensive application. Therefore, many researchers are searching for cheap and effective raw materials for the production of low-cost and highly efficient activated carbons. The literature contains studies on the removal of Cr (VI) by activated carbons produced from coconut shell [9], groundnut husk [10], *Casurina equisetifoli* leaves [11], used tyres and sawdust [12], etc.

Trapa natans L. (Trapaceae), also known as water chestnut, is an annual floating herb widely distributed in Asia including China and similar countries [13]. It is an important warm season crop in these regions and also a good commodity in the food industry because of its unique taste and high nutritive value [14]. The dark-brown corms (whole fruit) need to be peeled before cooking or canning, and the residual husk is often discarded or burned, which may cause water or air pollution. There are about 750–1000 tons of such husk produced per year just in the Nansi lake area (China) [15]. *T. natans* husk has a high content of C (43.4%), O (50.4%) and H (5.7%), which may offer a good basis for the production of an effective activated carbon. Therefore, making *T. natans* husk into activated carbon would not only avoid environmental problems but also make better use of this abundant and almost cost-free biomass material. However, to the best of our knowledge, no work

* Corresponding author. Tel.: +86 531 88363015; fax: +86 531 88364513.
E-mail address: zhangjian00@sdu.edu.cn (J. Zhang).

1385-8947/$ – see front matter © 2010 Elsevier B.V. All rights reserved.
doi:10.1016/j.cej.2010.06.020

Nomenclature

A_T	Tempkin equilibrium binding constant (L/min)
B	time constant of the Boyd model
B_T	Tempkin constant
C	intercept of the intra-particle diffusion model (mg/g)
C_e	equilibrium Cr (VI) concentration (mg/L)
C_i	initial Cr (VI) concentration (mg/L)
Di	effective diffusion coefficient (m^2/s)
F	represents the fraction of solute adsorbed at any time t (mg/g)
k_1	rate constant of the pseudo-first-order model (1/min)
k_2	rate constant of the pseudo-second-order model (g/(mg min))
K_C	Langmuir constant (L/mol)
k_{dif}	intra-particle diffusion rate constant (mg/(g $min^{0.5}$))
K_F	Freundlich constant representing adsorption capacity ((mg/g)(L/mg)$^{1/n}$)
k_L	Langmuir constant related to the apparent energy of adsorption (L/mg)
n	Freundlich exponent related to the adsorption intensity.
N	the number of experimental data points
Q_{cal}	Cr (VI) uptake amount calculated from kinetic or isotherm fitted models (mg/g)
Q_e	amount of Cr (VI) adsorbed at equilibrium (mg/g)
Q_{exp}	experimental Cr (VI) uptake amount (mg/g)
Q_m	maximum Langmuir adsorption capacity (mg/g)
Q_t	amount of Cr (VI) adsorbed at time t (mg/g)
r_0	radius of the adsorbent particle (m)
R	universal gas constant (8.314 J/(mol K))
R^2	correlation coefficients
t	contact time (min)
T	absolute temperature (K)
V	volume of the solution (L)
W	mass of the adsorbent (g)
ΔG^0	Gibbs free energy of adsorption (kJ/mol)
ΔH^0	enthalpy of adsorption (kJ/mol)
ΔS^0	entropy of adsorption (kJ/(mol K))
χ^2	non-linear chi-square test analysis

has been done so far on the use of *T. natans* husk for the preparation of activated carbon.

Fe oxides, especially amorphous forms, have a high affinity and selectivity toward Cr (VI) oxyanions [16] as well as anionic phosphorus and arsenic species. Impregnating iron (hydr)oxides into activated carbon can take advantage of both the high selectivity of ferric oxides for Cr (VI) and the high surface area of activated carbon which offers adequate reactive sites for iron loading. Several researchers have recently incorporated iron (hydr)oxides into activated carbon and thus greatly enhanced the arsenic adsorption capacity [17–19]. However, no studies have yet been published on the removal of Cr (VI) using Fe-loaded activated carbon.

In this research, we developed an iron-modified activated carbon using waste *T. natans* husk as precursor, and evaluated its ability to adsorb Cr (VI) from aqueous solutions. The objectives of this study were (1) to prepare and characterize a low-cost iron-modified activated carbon from *T. natans* husk (THAC-Fe); (2) to understand the adsorption behavior of THAC-Fe toward Cr (VI) by investigating the effect of experimental parameters such as pH, adsorbent dose and initial Cr (VI) concentration, as well as studying the adsorption kinetics, isotherms, thermodynamics and desorption characteristics of THAC-Fe.

2. Materials and methods

2.1. Chemicals

All the chemicals used were of analytical grade. A stock solution of chromium (VI) (100 mg/L) was prepared by dissolving 0.2829 g of $K_2Cr_2O_7$ in 1000 mL distilled water. Desired concentrations were obtained by diluting the stock solution with distilled water.

2.2. Preparation of THAC and THAC-Fe

T. natans husk (TH), obtained from the Nansi lake area in Shandong province, China, was washed with tap water, dried and ground in a laboratory mill, then dried again. The dried precursor was soaked in 45 wt% H_3PO_4 overnight at a ratio of 2.3:1 (H_3PO_4:TH, w/w), followed by carbonization and activation in a muffle furnace at 450 °C for 60 min, then allowed to cool naturally to room temperature. The produced material was washed with distilled water until a constant near neutral pH was observed, then dried at 105 °C for 8 h, allowed to cool to room temperature, and sieved to 140–200 mesh by standard sieves (Model Φ200). This particle size was chosen according to the literature [20,21], and the carbon powder obtained was quite fine and uniform in this range. The product was referred to as THAC.

Iron was incorporated into THAC as follows: 1.0 g of THAC was mixed with 400 mL of ferric chloride solution containing 100 ppm Fe^{3+} for 12 h, then the solid was separated from the solvent with a vacuum pump and washed with 800 mL water. The mass obtained was further dried at room temperature for 2 h and at 100 °C for 12 h. This iron-modified activated carbon was referred to as THAC-Fe. The iron content of THAC-Fe was 37.6 mg/g as calculated from the difference between the initial and final Fe^{3+} concentrations.

Based on the current commodity price in Shandong province, production of 1 kg THAC and THAC-Fe cost about US$ 0.45 and US$ 0.53 (including material and energy consumption), respectively. This price is relatively low as compared to the commonly used adsorbents for Cr (VI) removal such as activated alumina (US$ 0.66–1.19/kg), coconut shell-based activated carbon (US$ 0.88–1.32/kg) and coal-based activated carbon (US$ 0.54–0.71/kg) in China. In fact, the cost of THAC and THAC-Fe would be further reduced when applied in large-scale industrial production.

2.3. Characterization of THAC and THAC-Fe

The BET surface areas (S_{BET}) and porosities of THAC and THAC-Fe were measured based on N_2 adsorption/desorption isotherms at 77 K using a surface area analyzer (Quantachrome Corporation, USA). pore-size distribution was derived from BET and DFT methods. The surface area (S_{BET}) and the total pore volume (V_t) were obtained using the manufacturer's software. The external surface area (S_{ext}) and micropore surface area (S_{mic}), as well as the micropore volume (V_{mic}) were calculated by the t-plot method. The mean pore diameter, D_p, was deduced from $D_p = 4\,V_t/S_{BET}$.

The concentrations of acidic and basic functional groups on the carbon surface were determined by the Boehm titration method [22]. The pH at the point of zero charge (pH_{pzc}) was estimated from a batch equilibrium method described by Babic [23]. X-ray diffraction (XRD) patterns of the samples were obtained on a Rigaku D/MAX-RA diffraction with Ni-filtered Cu Kα radiation as X-ray source.

2.4. Adsorption experiments

Batch equilibrium Cr (VI) adsorption studies were performed by mixing a known dose of THAC or THAC-Fe (0.02–0.5 g) with 100 mL solutions of certain Cr (VI) concentration in a 250-mL Erlenmeyer flask, and the flasks were shaken at 300 rpm in a water bath shaker (SHZ-88) at 20 ± 1 °C for 8 h to reach equilibrium. Then the mixture was filtered and the residual Cr (VI) concentrations were measured according to the standard methods [24] using an UV–vis spectrophotometer (UV-754, Shanghai) at a wavelength of 540 nm. In pH studies, the initial solution pH was adjusted to 2–11 with 0.1 M HCl or 0.1 M NaOH solutions, and the pH values were measured by a pH meter (Model pHS-3C). Adsorption isotherm experiments were performed at 20, 30 and 40 °C. The uptake amount Q_e (mg/g) and removal efficiency of Cr (VI) at equilibrium can be calculated as follows:

$$Q_e = \frac{(C_i - C_e)V}{W} \quad (1)$$

$$\%\,\text{removal} = \frac{100(C_i - C_e)}{C_i} \quad (2)$$

where C_i and C_e (mg/L) are the initial and equilibrium concentrations of Cr (VI), respectively. V (L) is the volume of the solution and W (g) is the mass of THAC or THAC-Fe.

Adsorption kinetic experiments were done to investigate the effect of contact time and evaluate the kinetic properties. THAC-Fe (3.0 g) was added into 2000 mL of Cr (VI) solution with initial concentrations of 3.5, 10.0 or 20.0 mg/L. The mixture was agitated on an electromagnetic stirrer (Model 78-1) at 300 rpm and 20 ± 1 °C. The stirring rate of 300 rpm was chosen to disperse THAC-Fe homogenously in solution. At preset time intervals (0–480 min), 10 mL samples were drawn and filtered, and the residual chromium (VI) concentration was analyzed by the same method described above. The adsorption amount at time t (min), Q_t (mg/g), was obtained by

$$Q_t = \frac{(C_i - C_t)V}{W} \quad (3)$$

where C_i and C_t (mg/L) are the concentrations of Cr (VI) at initial and time t, respectively. V (L) is the solution volume and W (g) represents the amount of THAC-Fe used.

2.5. Desorption studies

Desorption studies were conducted using distilled water (pH ~ 6) and NaOH solutions of various concentrations (0.1–2.0 mol/L). After saturating THAC-Fe with Cr (VI) solution under the conditions: THAC-Fe dose = 0.15 g/100 mL, C_i = 10.0 mg/L, t = 8 h, the adsorbent was filtered and gently washed with distilled water to remove any unadsorbed chromium (VI) trapped between the adsorbent particles. Then the sample was immediately mixed with 100 mL of distilled water or NaOH solution, and agitated at 20 ± 1 °C for 16 h (previous work indicated that desorption could reach equilibrium after 12 h).

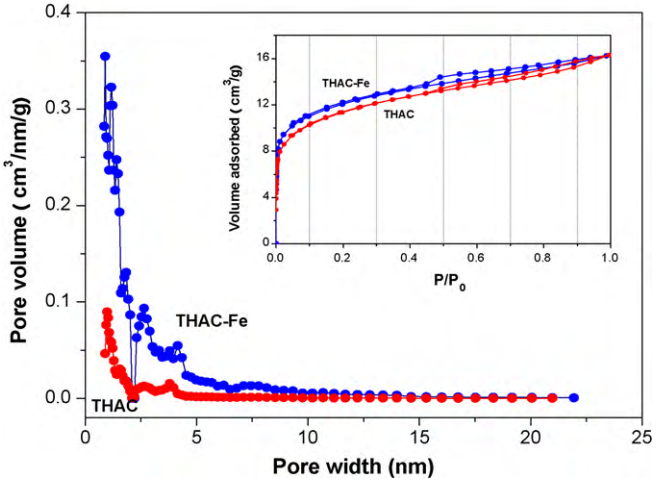

Fig. 1. Pore-size distributions of THAC and THAC-Fe. Inset is their N_2 adsorption/desorption isotherms.

3. Results and discussion

3.1. Characteristics of THAC and THAC-Fe

The THAC and THAC-Fe samples were essentially micro–mesoporous structures with most pores less than 5 nm, as shown by the pore-size distributions in Fig. 1. The N_2 adsorption/desorption isotherms for both samples (Fig. 1) showed a type IV curve, according to the IUPAC classification. THAC-Fe exhibited a high surface area and large total pore volume (Table 1). Impregnation with iron did not block the pores of the carbon, but increased the BET surface area by 17.5% and total pore volume by 24.1%. The increment in surface area and pore volume was more dramatic for mesopores than for micropores.

The results of the Boehm measurement of surface functional groups (Table 2) show that the total number of functional groups in THAC-Fe is almost equivalent to THAC, but there is an obvious variation in the types of groups. Iron impregnation introduced more acidic groups, especially carboxyls and phenols, but also sharply decreased the content of basic groups. It has been proposed that $FeCl_3$ is an oxidant and can provide or create more active sites (e.g. oxygen containing groups) on the carbon surface [25]. The increased acidic groups and decreased basic groups increase the overall surface acidity, which was also manifested by the results of pH_{pzc} measurement (Table 2).

Table 1
Surface areas and porosities of THAC and THAC-Fe.

Activated carbon	S_{BET} (m^2/g)	S_{ext}		S_{mic}		V_t (cm^3/g)	V_{mic}		D_p (nm)
		(m^2/g)	(%)	(m^2/g)	(%)		(cm^3/g)	(%)	
THAC	782.86	302.74	38.67	480.12	61.33	0.498	0.231	46.37	2.55
THAC-Fe	920.13	394.55	47.88	525.59	57.12	0.618	0.249	40.29	2.69

Table 2
Concentrations of surface functional groups and pH_{pzc} values of THAC and THAC-Fe.

Activated carbon	pH_{pzc}	Carboxylic groups (mmol/g)	Lactones (mmol/g)	Phenolic groups (mmol/g)	Acidic groups (mmol/g)	Basic groups (mmol/g)	Total groups (mmol/g)
THAC	6.20	0.83	0.36	0.75	1.94	1.51	3.45
THAC-Fe	3.77	1.70	0.60	1.08	3.38	0.11	3.49

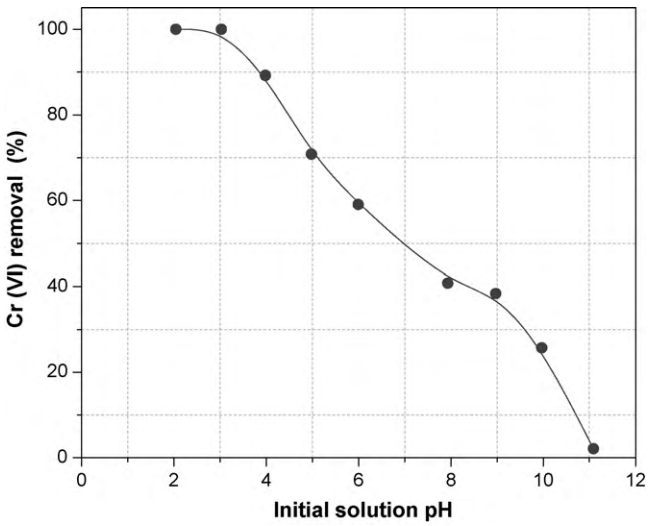

Fig. 2. Effect of initial solution pH on the removal of Cr (VI) by THAC-Fe (C_i = 10.0 mg/L; carbon dose = 0.8 g/L; temperature = 20 ± 1 °C).

No difference was observed between untreated THAC and that impregnated with Fe in terms of their XRD patterns. This result suggests that the iron impregnated into THAC was predominantly amorphous. Amorphous iron (hydr)oxides are known to gradually transfer to crystalline Fe (III) oxides [26], but this phenomenon did not take place for our samples. It could be that the impregnated iron is mostly coordinated with various functional groups on THAC, not in polymeric iron hydroxide form, so formation of crystalline iron (III) oxides was inhibited.

3.2. Effect of initial solution pH

The pH of the solution is considered to be the most important controlling parameter in the adsorption process. Fig. 2 depicts the effect of initial solution pH on the removal of Cr (VI) at a fixed initial Cr (VI) concentration of 10.0 mg/L and sorbent dose of 0.8 g/L. It is clear that the adsorption of Cr (VI) by THAC-Fe is highly pH dependent. The maximum removal efficiency (100%) occurred at pH 2–3, then the removal percentage decreased dramatically from 100% to 2.1% as the initial solution pH increased from 3 to 11. Similar observations have been reported by several investigators [27–30].

The chromate may be present in various forms in the solution phase as a function of pH and chromium concentration [31]:

$$H_2CrO_4 \leftrightarrow H^+ + HCrO_4^- \quad (4)$$

$$HCrO_4^- \leftrightarrow H^+ + CrO_4^{2-} \quad (5)$$

$$2HCrO_4^- \leftrightarrow Cr_2O_7^{2-} + H_2O \quad (6)$$

At solution pH of 2–3, the predominant Cr (VI) species is $HCrO_4^-$, but as the pH increases, this form shifts to $Cr_2O_7^{2-}$ and CrO_4^{2-}. $HCrO_4^-$ is more favorable for sorption since it has a low adsorption free energy [30]. The high removal efficiency at low pH can also be attributed to the fact that the surface of the adsorbent becomes highly protonated and positively charged below the pH_{pzc} (3.77), which favors the uptake of Cr (VI) anions through electrostatic attraction. An increase in the solution pH will make the surface less positively charged (negative when pH > pH_{pzc}), greatly weakening the electrostatic attraction between the sorbent and negatively charged Cr (VI) anions, thus reducing the removal efficiency. Moreover, as the pH increases, there is competition between OH^- and chromate ions, especially at high pH levels. It is also postulated that at low pH (<3) Cr (VI) can be reduced to Cr (III) in the presence of activated carbon [32]:

$$3C + 2Cr_2O_7^{2-} + 16H^+ = 3CO_2 + 4Cr^{3+} + 8H_2O \quad (7)$$

$$3C + 4CrO_4^{2-} + 20H^+ = 3CO_2 + 4Cr^{3+} + 10H_2O \quad (8)$$

Since the pH values of different wastewaters may vary, the adsorption studies below were conducted without adjusting the initial solution pH.

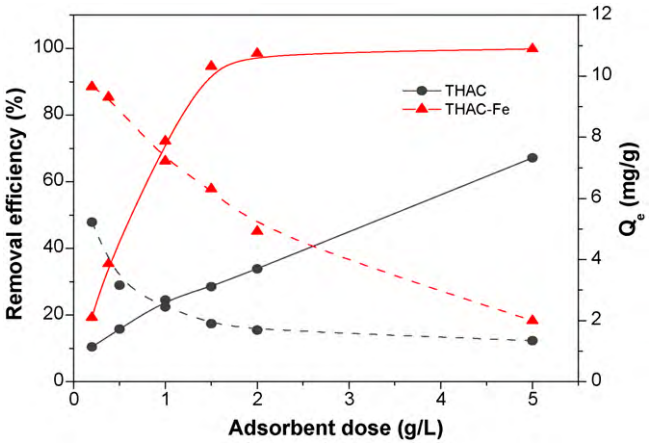

Fig. 3. Effect of adsorbent dose on the adsorption of Cr (VI) by THAC-Fe and THAC (C_i = 10.0 mg/L; temperature = 20 ± 1 °C; pH 6.0). The dotted lines and solid lines correspond to Q_e and Cr (VI) removal efficiency, respectively.

3.3. Effect of adsorbent dose

The effect of THAC-Fe and THAC dose on the adsorption of Cr (VI) from aqueous solutions was investigated using various adsorbent doses (0.2–5.0 g/L) at a constant chromium (VI) concentration of 10.0 mg/L. As shown in Fig. 3, the removal efficiency of Cr (VI) by THAC-Fe increased sharply as the sorbent dose increased from 0.2 to 1.5 g/L, then reached an almost constant value of 99.8%. However, as expected, the adsorption capacities decreased with increasing adsorbent mass, due to the reduction in both effective surface area and adsorbate/adsorbent ratio. The removal efficiency was 94.6% when the THAC-Fe dose was 1.5 g/L, beyond which the removal was not significantly increased, so 1.5 g/L was chosen as the optimum adsorbent dose for further experiments.

As compared to THAC-Fe, THAC exhibited much lower removal efficiency and adsorption capacity for Cr (VI), which was about one third of the former at a sorbent dose of 1.5 g/L. Impregnation with iron significantly enhances the adsorption capacity of the activated carbon toward chromium (VI). This improvement can be explained as follows: THAC-Fe possesses much larger surface area and micropore and mesopore volumes than THAC. Iron impregnation also introduces more acidic functional groups such as carboxyls, lactones and phenols to the carbon surface, which can provide more adsorption sites for Cr (VI) and enhance the adsorption capacity [29]. Furthermore, the iron oxides contained in THAC-Fe have high affinity and selectivity toward Cr (VI) oxyanions, and they may contribute to the chromium adsorption.

3.4. Effect of contact time and initial Cr (VI) concentration

Fig. 4 shows the relation between Cr (VI) uptake and contact time at different initial chromium concentrations of 3.5, 10.0 and 20.0 mg/L. The adsorption showed a rapid increase during the first 40 min for all concentrations, which is probably because adequate vacant sites are available and a great concentration gradient exists between the adsorbate in aqueous and solid phases. Thereafter the rate of adsorption was found to be slow and finally approached

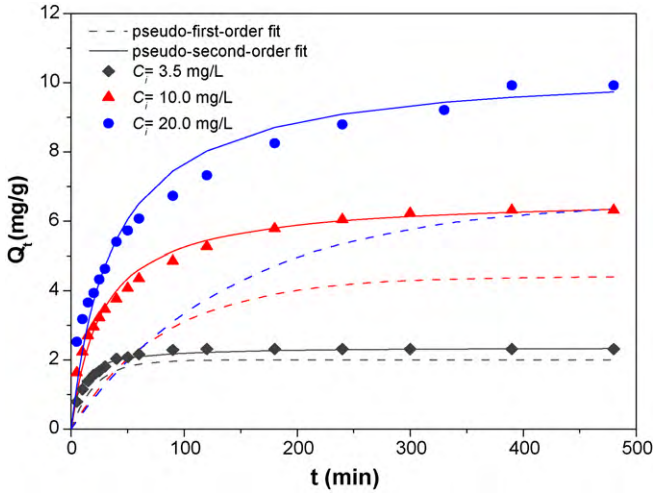

Fig. 4. Effect of contact time and comparison of different kinetic models for Cr (VI) adsorption onto THAC-Fe at three different initial concentrations (carbon dose = 1.5 g/L; temperature = 20 ± 1 °C; pH 6.0).

equilibrium. For 3.5 mg/L Cr (VI), 2.31 mg Cr (VI)/g THAC-Fe was adsorbed after equilibrating for only 90 min. But for 10 mg/L Cr (VI), 6.32 mg/g was adsorbed after 300 min and for 20 mg/L Cr (VI), a maximum of 9.93 mg/g was adsorbed after equilibrating for 390 min. It is evident that an increase in the initial Cr (VI) concentration led to a notable increase in the equilibrium time and adsorption amount. However, the removal percent of Cr (VI) decreased from 99.0% to 74.5% as Cr (VI) initial concentrations increased from 3.5 to 20.0 mg/L. Therefore, the adsorption of Cr (VI) by THAC-Fe has a strong dependence on the initial concentration.

3.5. Adsorption kinetics

Adsorption kinetics data were analyzed by the two most widely used kinetic models, i.e. the pseudo-first-order and pseudo-second-order model. The linear form of the pseudo-first-order equation [10] can be expressed as

$$\ln(Q_e - Q_t) = \ln Q_e - k_1 t \tag{9}$$

where Q_e and Q_t (mg/g) are the amounts of Cr (VI) adsorbed at equilibrium and at time t (min), respectively, and k_1 (1/min) is the rate constant of the pseudo-first-order model. The values of Q_e and k_1 can be obtained from the intercept and slope of a plot of $\ln(Q_e - Q_t)$ versus t.

The linear form of the pseudo-second-order equation [30] is given as follows:

$$\frac{t}{Q_t} = \frac{1}{k_2 {Q_e}^2} + \frac{1}{Q_e} t \tag{10}$$

where k_2 (g/(mg min)) is the pseudo-second-order rate constant. The parameters Q_e and k_2 can be estimated from the slope and the intercept of the plot (t/Q_t) versus t.

The best-fitting model was determined by the correlation coefficients (R^2), together with a non-linear chi-square test analysis (χ^2), which is defined as [31]:

$$\chi^2 = \sum \frac{(Q_{exp} - Q_{cal})^2}{Q_{cal}} \tag{11}$$

where Q_{exp} and Q_{cal} (mg/g) are the experimental and calculated uptake amounts of Cr (VI) by THAC-Fe. A smaller χ^2 value means little deviation between the values calculated from the model and the experimental data.

The comparison of different kinetic models for the adsorption of Cr (VI) onto THAC-Fe at different initial concentrations is plotted in Fig. 4. All kinetic parameters, correlation coefficients and χ^2 are listed in Table 3. As seen from Fig. 4, the pseudo-first-order model did not show a good agreement to the experimental kinetic data, this can also be concluded from the low R^2 and large χ^2 values. However, the pseudo-second-order model fit the experimental data quite well with all correlation coefficients R^2 higher than 0.994, and good agreements between Q_{cal} and Q_{exp}, so it is an ideal model to describe the adsorption of Cr (VI) by THAC-Fe. The values of the rate constant k_2 decreased markedly as the initial Cr (VI) concentration increased.

3.5.1. Intra-particle diffusion model

Adsorption of any metal ion from aqueous phase onto porous materials proceeds by a multi-step process, and the procedure is usually controlled by either the film diffusion (external mass transfer) or the intra-particle diffusion rate or both [8]. In order to identify the diffusion mechanism, the intra-particle diffusion model is explored by the following equation [33]:

$$Q_t = k_{dif} t^{0.5} + C \tag{12}$$

where Q_t (mg/g) is the amount of Cr (VI) adsorbed at time t (min), k_{dif} (mg/(g min$^{0.5}$)) is the intra-particle diffusion rate constant and C (mg/g) is the intercept, which represents the thickness of the boundary layer. A larger C value means a greater effect of the boundary layer [33].

Intra-particle diffusion is the sole rate-limiting step if the plot of Q_t versus $t^{0.5}$ is a straight line that passes through the origin [34]. However, the plots obtained from this study (Fig. 5) presented

Table 3
Pseudo-first-order, pseudo-second-order and Intra-particle diffusion kinetic parameters for the adsorption of Cr (VI) by THAC-Fe.

Kinetic models	Parameters	3.5 mg/L	10.0 mg/L	20.0 mg/L
Pseudo-first-order	k_1 (1/min)	0.0474	0.0124	0.0072
	Q_{cal} (mg/g)	2.00	4.41	6.56
	R^2	0.9877	0.9835	0.9839
	χ^2	1.3558	41.3890	121.5667
Pseudo-second-order	k_2 (g/(mg min))	0.0550	0.0056	0.0026
	Q_{cal} (mg/g)	2.43	6.69	10.48
	R^2	0.9991	0.9988	0.9947
	χ^2	0.1064	0.5289	2.0372
Intra-particle diffusion [a]	k_{dif} (mg/(g min$^{0.5}$))	0.0832	0.3302	0.3575
	C (mg/g)	1.503	1.7045	3.3541
	R^2	0.9851	0.9928	0.9950
	χ^2	0.0003	0.0039	0.0031
Q_{exp} (mg/g)		2.31	6.32	9.93

[a] Parameters for the second portion of the intra-particle diffusion curves.

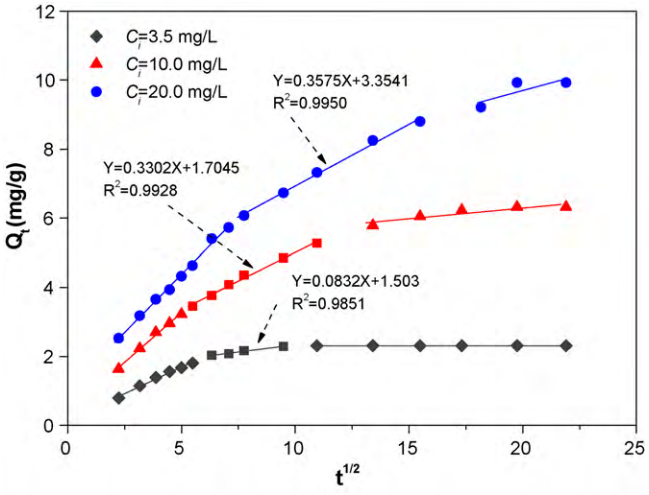

Fig. 5. Intra-particle diffusion plots for Cr (VI) adsorption onto THAC-Fe at three different initial concentrations (carbon dose = 1.5 g/L; temperature = 20 ± 1 °C; pH 6.0).

multi-linearity, indicating that two or more steps occur during the adsorption process. The initial sharper portion was the external surface adsorption or the instantaneous adsorption. The second portion was the gradual adsorption stage where intra-particle diffusion was rate-limiting (straight lines with $R^2 > 0.98$ as given in Table 3). The third portion was the final equilibrium stage where intra-particle diffusion started to slow down due to the extremely low adsorbate concentrations left in the solutions [35]. The multi-linearity of the curves suggests that both surface adsorption and intra-particle diffusion were simultaneously occurring during the process and contribute to the adsorption mechanism. However, still there is no sufficient indication about which of the two steps is the rate-limiting step of the whole process.

The values of k_{dif} and C reported in Table 3 were calculated according to the second portion of the curves. The C values increased with the initial Cr (VI) concentration, which indicated an increase of the thickness of the boundary layer and therefore internal mass transfer is favored over external mass transfer [36]. The intra-particle diffusion rate constant, k_{dif}, increased from 0.08 to 0.36 mg/(g min$^{0.5}$) as the initial chromium concentration increased from 3.5 to 20 mg/L.

3.5.2. Boyd model

In order to determine the slowest step in the overall adsorption process, the sorption data were further analyzed by the kinetic expression given by Boyd et al. [37]:

$$F = 1 - \frac{6}{\pi^2}\sum_{N=1}^{\infty}\frac{1}{N^2}\exp[-N^2Bt] \quad (13)$$

where F represents the fractional attainment of equilibrium at time t (min), and is obtained by the value of Q_t/Q_e, where Q_t and Q_e (mg/g) are the uptake amounts of Cr (VI) at time t and equilibrium, respectively. N is the number of experimental data points. B is the time constant.

Bt values can be obtained for each observed value of F, using Reichenberg's table [38]. If the plot of Bt versus t is a straight line passing through the origin, then the rate-limiting step in the adsorption process is the intra-particle diffusion, and vice versa.

Table 4
Langmuir, Tempkin and Freundlich isotherms and their linear forms.

Isotherms	Langmuir[a,b]	Tempkin[a,b]	Freundlich[a,b]
Isotherm theory	Monolayer adsorption on homogenous sites; uniform energies of adsorption onto the surface.	Adsorbate–adsorbate interaction; uniform distribution of maximum binding energy.	Adsorption on heterogeneous surfaces; interaction between adsorbed molecules.
Non-linear form	$Q_e = Q_m k_L C_e/(1 + k_L C_e)$	$Q_e = B_T \ln(A_T C_e)$	$Q_e = K_F C_e^{1/n}$
Linear form	$C_e/Q_e = (1/Q_m k_L) + (1/Q_m)C_e$	$Q_e = B_T \ln A_T + B_T \ln C_e$	$\ln Q_e = \ln K_F + (1/n)\ln C_e$
Plot	C_e/Q_e vs. C_e	Q_e vs. $\ln C_e$	$\ln Q_e$ vs. $\ln C_e$
Parameters	k_L (L/mg) – Langmuir constant related to the apparent energy of adsorption; Q_m (mg/g) – the maximum monolayer adsorption capacity.	B_T – Tempkin constant; A_T (L/min) – the equilibrium binding constant.	K_F ((mg/g)(L/mg)$^{1/n}$) – Freundlich constant representing adsorption capacity; n – Freundlich exponent related to the adsorption intensity.

[a] Q_e (mg/g) – Cr (VI) uptake at equilibrium.
[b] C_e (mg/L) – Cr (VI) concentration at equilibrium.

Table 5
Langmuir, Tempkin and Freundlich isotherm parameters for the adsorption of Cr (VI) by THAC-Fe at different temperatures.

Isotherms	Parameters	20 °C	30 °C	40 °C
Langmuir	Q_m (mg/g)	11.834	14.493	18.657
	k_L (L/mg)	14.322	10.454	89.332
	R^2	0.9939	0.9947	0.9930
	χ^2	1.198	10.812	5.448
Tempkin	B_T	1.188	1.191	1.947
	A_T	7382.988	33291.705	35151.049
	R^2	0.9536	0.9168	0.9738
	χ^2	0.088	0.193	0.081
Freundlich	K_F ((mg/g)(L/mg)$^{1/n}$)	10.508	12.258	21.822
	n	7.582	9.363	7.047
	R^2	0.9416	0.9489	0.9909
	χ^2	0.102	0.110	0.036

Table 6
Adsorption capacities of various low-cost adsorbents for Cr (VI).

Adsorbent	Q_m (mg/g)	Sorbent dose (g/L)	Reference
Coconut shell carbon	10.88	1.5	[9]
Sawdust activated carbon	3.46	4	[12]
Cationic surfactant-modified activated carbon	1.819	10	[42]
Granular activated carbon	0.988	5	[43]
Almond	10.62	8	[44]
Coal	6.78	8	[44]
Cactus	7.08	8	[44]
Raw rice bran	0.07	10	[45]
Sunflower stem	4.9	4	[46]
Coaly activated carbon	8.77	5	[47]
Sulfur acid-modified waste activated carbon	7.49	2	[48]
Fe-modified *Trapa natans* husk activated carbon	11.83	1.5	This work

The plots obtained in this study were linear but did not pass though the origin, indicating that film diffusion is the rate-controlling step in the adsorption process.

The effective diffusion coefficient D_i (cm^2/s) can be calculated by the obtained B values and the radius of the adsorbent particle r_0 (m) using the relation:

$$B = \frac{\pi^2 D_i}{{r_0}^2} \tag{14}$$

The D_i values were found to be 6.33×10^{-8}, 1.54×10^{-8}, and 0.96×10^{-8} cm^2/s, respectively for initial Cr (VI) concentrations of 3.5, 10.0 and 20.0 mg/L, which indicates that the Cr (VI) adsorption onto THAC-Fe has a lower film diffusion rate constant at higher initial concentrations.

3.6. Adsorption isotherms and thermodynamics

Adsorption isotherms provide qualitative information on the capacity of the adsorbent as well as the nature of the solute–surface interaction. In this study, equilibrium data at various temperatures (20, 30, 40 °C) were analyzed by three empirical adsorption models, namely Langmuir [39], Tempkin [40] and Freundlich [41] isotherms, the non-linear and linear forms of which are displayed in Table 4.

According to the fitting results listed in Table 5, the correlation coefficients of the three models were always higher than 0.91. However, when χ^2 were considered, the Tempkin and Freundlich isotherms appeared to be much more applicable than the Langmuir isotherm model, due to their much smaller χ^2 values. Therefore the uptake of Cr (VI) by THAC-Fe may involve a multi-molecular layer adsorption with interactions between the adsorbed molecules, and the surface of THAC-Fe is relatively heterogeneous.

As shown in Table 5, the n values were higher than 1.0 for all temperatures, indicating that Cr (VI) adsorption onto THAC-Fe is favorable [41]. Q_m and K_F values increased with the increasing temperature, suggesting that the adsorption is endothermic. A comparison of the adsorption capacities for Cr (VI) by other low-cost adsorbents is given in Table 6. The high adsorption capacity of this study revealed that THAC-Fe could be a promising adsorbent for Cr (VI) removal.

3.6.1. Adsorption thermodynamics

Thermodynamic parameters including changes in the Gibbs free energy (ΔG^0, kJ/mol), enthalpy (ΔH^0, kJ/mol), and entropy (ΔS^0, kJ/(mol K)) during the adsorption process are determined by the following equations [42]:

$$\Delta G^0 = -RT \ln K_C \tag{15}$$

Table 7
Thermodynamic parameters for the adsorption of Cr (VI) by THAC-Fe.

T (°C)	ΔG^0 (kJ/mol)	ΔH^0 (kJ/mol)	ΔS^0 (kJ/(mol K))
20	−32.94		
30	−33.27	70.844	−0.3506
40	−39.95		

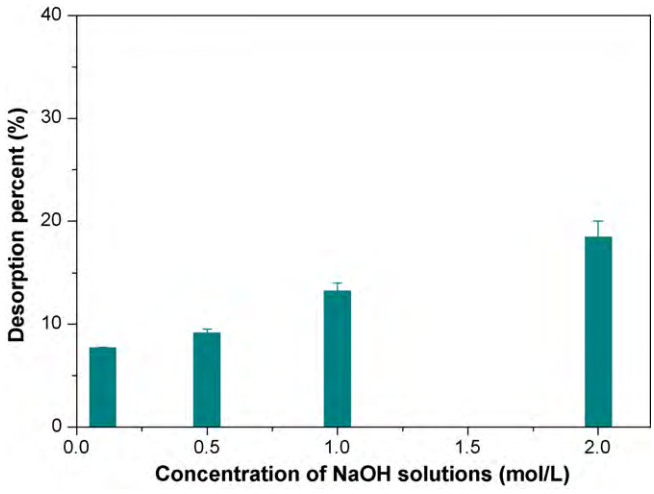

Fig. 6. Cr (VI) desorption efficiency from the Cr (VI)-loaded THAC-Fe by NaOH solutions of various concentrations.

$$\Delta G^0 = \Delta H^0 - T\Delta S^0 \tag{16}$$

where R (8.314 J/(mol K)) is the gas constant, T (K) is the absolute temperature, and K_C (L/mol) is the Langmuir constant obtained from the plot of C_e/Q_e vs. C_e. The ΔH^0 and ΔS^0 values can be calculated from the intercept and slope of the plot of ΔG^0 vs. T, respectively. The values of these parameters are recorded in Table 7. The free energy changes (ΔG^0) were negative, indicating the spontaneity and feasibility of the process. More negative ΔG^0 values at higher temperature showed that an increase in temperature favored the adsorption. The positive value of ΔH^0 further confirmed the endothermic nature of the adsorption. The negative value of ΔS^0 accords with the fact that the mobility of the adsorbate was more restricted on the adsorbent surface than in solution [41].

3.7. Desorption studies

Desorption studies help to determine the adsorption mechanism and to evaluate the feasibility of regenerating the spent activated carbon. The results of the desorption experiments are depicted in Fig. 6. No Cr (VI) recovery was observed when distilled water was used to desorb Cr (VI) from Cr (VI)-loaded THAC-Fe. There was also very little desorption (7.7–18.4%) with 0.1–2.0 mol/L NaOH solutions. These findings imply that the mechanism of chromium (VI) adsorption onto THAC-Fe is predominantly chemisorption, and the Cr (VI) ions may have formed strong bonds with the adsorbent surface [49].

4. Conclusions

In this study, Fe-modified activated carbon prepared from *T. natans* husk, a cheap aquatic plant residue, proved to be an effective adsorbent for Cr (VI) removal from wastewater. THAC-Fe has a higher surface area, lower pH_{pzc}, more acidic functional groups and superior adsorption capacity as compared to THAC alone. The adsorption of Cr (VI) by THAC-Fe was most favorable under acidic

conditions. The adsorption system followed pseudo-second-order kinetics. The rate of Cr (VI) uptake was found to be controlled by both external mass transfer and intra-particle diffusion. Boyd plot indicated that external mass transfer was the rate-limiting step in the adsorption process. Experimental equilibrium data were in good agreement with the Tempkin and Freundlich models. The maximum adsorption capacity was 11.83 mg/g as calculated by Langmuir equation. Thermodynamic parameters (ΔG^0, ΔH^0, ΔS^0) showed that the adsorption was feasible, spontaneous and endothermic. According to the desorption results, chemisorption is considered to be the mode of adsorption.

Acknowledgements

The work was supported by the National Key Technology R&D Program for the 11th Five-year Plan (No. 2006BAC10B03), the National Water Special Project (2009ZX07210-009-04) and Graduate Independent Innovation Foundation of Shandong University (2009JQ009). The authors thank Dr. Pamela Holt for editing the manuscript.

References

[1] K.C.K. Lai, I.M.C. Lo, Removal of chromium (VI) by acid-washed zero-valent iron under various groundwater geochemistry conditions, Environ. Sci. Technol. 42 (4) (2008) 1238–1244.
[2] N. Kongsricharoern, C. Polprasert, Chromium removal by a bipolar electrochemical precipitation process, Water Sci. Technol. 34 (1996) 109–116.
[3] C.A. Kozlowski, W. Walkowiak, Removal of chromium (VI) from aqueous solutions by polymer inclusion membranes, Water Res. 36 (2002) 4870–4876.
[4] S. Rengaraj, K.H. Yeon, S.H. Moon, Removal of chromium from water and wastewater by ion exchange resins, Hazard. Mater. B 87 (2001) 273–287.
[5] D. Mohan, K.P. Singh, V.K. Singh, Removal of hexavalent chromium from aqueous solution using low-cost activated carbons derived from agricultural waste materials and activated carbon fabric cloth, Ind. Eng. Chem. Res. 44 (4) (2005) 1027–1042.
[6] V.K. Gupta, A.K. Shrivastava, N. Jain, Biosorption of chromium (VI) from aqueous solutions by green algae Spirogyra species, Water Res. 35 (2001) 4079–4085.
[7] A. Baran, E. Bıçak, Ş. Hamarat-Baysal, S. Önal, Comparative studies on the adsorption of Cr (VI) ions on to various sorbents, Bioresour. Technol. 98 (2006) 661–665.
[8] R.L. Tseng, S.K. Tseng, Pore structure and adsorption performance of the KOH-activated carbons prepared from corncob, J. Colloid Interf. Sci. 87 (2005) 428–437.
[9] S. Babel, T.A. Kurniawan, Cr (VI) removal from synthetic wastewater using coconut shell charcoal and commercial activated carbon modified with oxidizing agents and/or chitosan, Chemosphere 54 (2004) 951–967.
[10] K. Periasamy, K. Srinivasan, P.R. Murugan, Studies on chromium (VI) removal by activated groundnut husk carbon, Ind. J. Environ. Health 33 (1991) 433–439.
[11] K. Ranganathan, Chromium removal by activated carbons prepared from *Casurina equisetifolia* leaves, Bioresour. Technol. 73 (2000) 99–103.
[12] N.K. Hamadi, X.D. Chen, M.M. Farid, M.G.Q. Lu, Adsorption kinetics for the removal of chromium (VI) from aqueous solution by adsorbents derived from used tyres and sawdust, Chem. Eng. J. 84 (2001) 95–105.
[13] G.D. Singh, R. Sharma, A.S. Bawa, D.C. Saxena, Drying and rehydration characteristics of water chestnut (*Trapa natans*) as a function of drying air temperature, J. Food Eng. 87 (2008) 213–221.
[14] M.L. Parker, K.W. Waldron, Texture of Chinese water chestnut: involvement of cell wall phenolics, J. Sci. Food Agric. 68 (1995) 337–346.
[15] B. Wang, X. Mu, J. Zhang, G. Shao, Effect of cultivar and ecological environment on the production of *Trapa natans*, Chin. Fruit Veg. 9 (2009) 18–19.
[16] Y.M. Tzou, M.K. Wang, R.H. Loeppert, Sorption of phosphate and Cr (VI) by Fe (III) and Cr (III) hydroxides, Arch. Environ. Contam. Toxicol. 44 (2003) 445–453.
[17] B.E. Reed, R. Vaughan, L.Q. Jiang, As (III), As (V), Hg, and Pb removal by Fe-oxide impregnated activated carbon, J. Environ. Eng. ASCE 126 (2000) 869–873.
[18] Z.M. Gu, J. Fang, B.L. Deng, Preparation and evaluation of GAC-based iron-containing adsorbents for arsenic removal, Environ. Sci. Technol. 39 (2005) 3833–3843.
[19] V. Fierroa, G. Muñiz, G. Gonzalez-Sánchezc, M.L. Ballinasb, A. Celzarda, Arsenic removal by iron-doped activated carbons prepared by ferric chloride forced hydrolysis, J. Hazard. Mater. 168 (2009) 430–437.
[20] J. Acharya, J.N. Sahu, B.K. Sahoo, C.R. Mohanty, B.C. Meikap, Removal of chromium (VI) from wastewater by activated carbon developed from tamarind wood activated with zinc chloride, Chem. Eng. J. 150 (2009) 25–39.
[21] J. Zhang, Q. Shi, C. Zhang, J. Xu, B. Zhai, B. Zhang, Adsorption of Neutral Red onto Mn-impregnated activated carbons prepared from *Typha orientalis*, Bioresour. Technol. 99 (2008) 8974–8980.
[22] H.P. Boehm, Some aspects of the surface chemistry of carbon blacks and other carbons, Carbon 32 (1994) 759–769.
[23] B.M. Babic, S.K. Milonjic, M.J. Polovina, B.V. Kaludierovic, Point of zero charge and intrinsic equilibrium constants of activated carbon cloth, Carbon 37 (1999) 477–481.
[24] China Bureau of Environmental Protection, Water and Wastewater Monitor and Analysis Method, fourth ed., China Environmental Science Press, Beijing, 2004.
[25] H. Cui, S.Q. Turn, Adsorption/desorption of dimethylsulfide on activated carbon modified with iron chloride, Appl. Catal. B: Environ. 88 (2009) 25–31.
[26] Y. Deng, W. Stumm, Reactivity of aquatic iron (III) oxyhydroxides—implications for redox cycling of iron in natural waters, Appl. Geochem. 9 (1994) 23–36.
[27] H. Demiral, İ. Demiral, F. Tümsek, B. Karabacakoğlu, Adsorption of chromium (VI) from aqueous solution by activated carbon derived from olive bagasse and applicability of different adsorption models, Chem. Eng. J. 144 (2008) 188–196.
[28] N.R. Bishnoi, M. Bajaj, N. Sharma, A. Gupta, Adsorption of Cr (VI) on activated rice husk carbon and activated alumina, Bioresour. Technol. 91 (2004) 305–307.
[29] D. Aggarwal, M. Goyal, R.C. Bansal, Adsorption of chromium by activated carbon from aqueous solution, Carbon 37 (1999) 1989–1997.
[30] P. Yuan, M. Fan, D. Yang, H. He, D. Liu, A. Yuan, J. Zhu, T. Chen, Montmorillonite-supported magnetite nanoparticles for the removal of hexavalent chromium from aqueous solutions, J. Hazard. Mater. 166 (2009) 821–829.
[31] L.V.A. Gurgel, J.C. Perin de Melo, J.C. de Lena, L.F. Gil, Adsorption of chromium (VI) ion from aqueous solution by succinylated mercerized cellulose functionalized with quaternary ammonium groups, Bioresour. Technol. 100 (2009) 3214–3220.
[32] A.S. Mestre, J. Pires, J.M.F. Nogueira, A.P. Carvalho, Activated carbons for the adsorption of ibuprofen, Carbon 45 (2007) 1979–1988.
[33] W.J. Weber, J.C. Morris, Kinetics of adsorption on carbon from solution, J. Sanit. Eng. Div. Am. Soc. Civil Eng. 89 (1963) 31–60.
[34] Ö. Gerçel, A. Özcan, A.S. Özcan, H.F. Gerçel, Preparation of activated carbon from a renewable bio-plant of *Euphorbia rigida* by H_2SO_4 activation and its adsorption behavior in aqueous solutions, Appl. Surf. Sci. 253 (2007) 4843–4852.
[35] F.C. Wu, R.L. Tseng, R.S. Juang, Comparisons of porous and adsorption properties of carbons activated by steam and KOH, J. Colloid Interf. Sci. 28 (2005) 49–56.
[36] A. El Nemr, A. Khaled, O. Abdelwahab, A. El-Sikaily, Treatment of wastewater containing toxic chromium using new activated carbon developed from date palm seed, J. Hazard. Mater. 152 (2008) 263–275.
[37] G.E. Boyd, A.W. Adamson, L.S. Meyers, The exchange adsorption of ions from aqueous solutions by organic zeolites. II. kinetics, J. Am. Chem. Soc. 69 (1947) 2836–2848.
[38] D. Reichenberg, Properties of ion-exchange resins in relation to their structure. III. Kinetics of exchange, J. Am. Chem. Soc. 75 (1953) 589–592.
[39] I. Langmuir, The adsorption of gases on plane surfaces of glass, mica and platinum, J. Am. Chem. Soc. 40 (1918) 1361–1403.
[40] M.I. Tempkin, V. Pyzhev, Kinetic of ammonia synthesis on promoted iron catalysts, J. Acta Physiochim. URSS 12 (1940) 327–356.
[41] H. Freundlich, Adsorption in solution, J. Phys. Chem. Soc. 40 (1906) 1361–1368.
[42] H.D. Choi, W.S. Jung, J.M. Cho, B.G. Ryu, J.S. Yang, K. Baek, Adsorption of Cr (VI) onto cationic surfactant-modified activated carbon, J. Hazard. Mater. 166 (2009) 642–646.
[43] H.D. Choi, J.M. Cho, K. Baek, J.S. Yang, J.Y. Lee, Influence of cationic surfactant on adsorption of Cr (VI) onto activated carbon, J. Hazard. Mater. 161 (2009) 1565–1568.
[44] M. Dakiky, M. Khamis, A. Manassra, M. Mer'eb, Selective adsorption of chromium (VI) in industrial wastewater using low-cost abundantly available adsorbents, Adv. Environ. Res. 6 (2002) 533–540.
[45] E.A. Oliveira, S.F. Montanher, A.D. Andrade, J.A. Nóbrega, M.C. Rollemberg, Equilibrium studies for the sorption of chromium and nickel from aqueous solutions using raw rice bran, Process Biochem. 40 (2005) 3485–3490.
[46] M. Jain, V.K. Garg, K. Kadirvelu, Chromium (VI) removal from aqueous system using *Helianthus annuus* (sunflower) stem waste, J. Hazard. Mater. 162 (2009) 365–372.
[47] Y. Wu, B. Li, S. Feng, X. Mi, J. Jiang, Adsorption of Cr (VI) and As (III) on coaly activated carbon in single and binary systems, Desalination 249 (2009) 1067–1073.
[48] P.K. Ghosh, Hexavalent chromium [Cr (VI)] removal by acid modified waste activated carbons, J. Hazard. Mater. 171 (2009) 116–122.
[49] D. Nityanandi, C.V. Subbhuraam, Kinetics and thermodynamic of adsorption of chromium (VI) from aqueous solution using puresorbe, J. Hazard. Mater. 170 (2009) 876–882.